Aria of the Dutch North Sea

Sertlek, H.O.; Sertlek H.O.

3.4. SOURCE SPECIFIC SOUND MAPPING: SPATIAL, TEMPORAL AND SPECTRAL DISTRIBUTION OF SOUND IN A HEAVILY EXPLOITED SEA

This section will be submitted as "H.Ö. Sertlek, H. Slabbekoorn, C. ten Cate and M.A. Ainslie, Source specific sound mapping: spatial, temporal and spectral distribution of sound in a heavily exploited sea "

Abstract: *Effective measures for protecting and preserving the marine environment require an understanding of the potential effect of sound on marine life. This section focuses on modelling the spatial, temporal and spectral distribution of the sound from the main sound sources in the Dutch North Sea in various frequency bands between 100 Hz and 100 kHz. The selected sound sources (shipping, airguns, underwater explosions and wind) are ranked according to their contribution to the total acoustic energy in the Dutch North Sea. Of these sources, shipping is predicted to be responsible for the largest amount of acoustic energy, (~400 J), followed by seismic surveys (~90 J), explosions (~80 J), and wind (~20 J), in the 100 Hz to 100 kHz frequency band, averaged over a two year period. The potential impact of these sounds on aquatic animals depends not only on these temporally averaged and spatially integrated broadband energies, but also on the source-specific spatial, spectral and temporal variation. Shipping is dominant in the southern part and along the coast in the north, throughout the years and across the spectrum. Seismic surveys are relatively local and spatially and temporally dependent on exploration activities in any particular year and spectrally more biased to low frequencies than the other sources. Explosions occur mainly in the southern part of the North Sea and contribute energy across the spectrum, but for very short point events in time. Wind is ubiquitous and omnipresent, though more prominent in the winter months and in the high frequency range. This variation needs to be taken into account when assessing the sound impact on marine life.*

3.4.1. INTRODUCTION

Sound is likely to play a dominant role in the life of aquatic animals in deep and dark oceans or shallow and murky waters, as well as in the bright and colourful world around coral reefs, [Myrberg and Fuiman 2002; Montgomery et al. 2006; Slabbekoorn et al. 2010]. Visibility in water is less than 40 meters even in the most optimal conditions, depending on depth, time of day and water turbidity [Mobly 1994; Trees et al. 2005]. Typically, water transparency is not optimal and available light can be weak in the deep, in shadows, or at night. Dissolved odours can provide information about habitat, presence of predators and prey or food in general, and may also serve a role in communication among conspecifics [McLennan 2003; Huijbers et al. 2008]. However, independent of conditions for vision and smell, but dependent on species-specific sensory abilities, sound often provides critical information about the environment to an organism, either by itself or in concert with other stimuli [Stevens 2013; Halfwerk and Slabbekoorn 2015].

Many aquatic animals rely on sound for various functions that are vital to survival and reproduction. Reasons for this are that sound propagates extremely well through water and that perception is independent of light conditions (e.g. in dark murky water or at night) or directional attention. Animals are known to communicate acoustically underwater or exploit environmental sounds to find prey, avoid predators, or for orientation [Slabbekoorn and Bouton,2008; Fay 2009]. However, biologically relevant sounds need to be extracted from a typically noisy background of many other sounds, which requires that animals are able to discriminate and recognize the relevant sounds. This ability will depend critically on suitable signal-to-noise ratios. Furthermore, the introduction of anthropogenic noise to the naturally present environmental sounds may not only increase the potential for masking problems, but also adds the possibly detrimental effects of distraction, disturbance, deterrence and injury [Popper and Hastings 2009; Slabbekoorn et al. 2010; Radford et al. 2014].

International concern about possible effects of anthropogenic sound sources on marine life has arisen due to increasing shipping traffic, exploitation of oil and gas reserves and the development of new offshore energy sources. This concern has led governments to introduce regulatory measures worldwide [Lucke et al 2014]. For example, the European Union's Marine Strategy Framework Directive (MSFD) [EU 2008] requires EU member states to achieve or maintain Good Environmental Status (GES) by 2020. Specifically, GES Descriptor 11 requires underwater noise to be "at levels that do not adversely affect the marine environment". The use of sound maps to

monitor and evaluate is the specific advice of a technical workgroup of the European Union on underwater noise (TSG Noise) [Dekeling et al,2014].

Sound maps can provide insight into the distribution of sound and the contribution to the energy budget from anthropogenic and natural sound sources. Many countries have an interest to identify the components of sound in their local seas [Dekeling et al 2014, Tyack et al,2015 ;Sutton et al, 2011; Folegot, 2012; Sertlek et al, 2015b, Cetsound; Hatch and Fristrup, 2009]. Sound maps can also provide insight and overview of the distribution and origins of sound for globally present sound sources such as shipping lanes [Porter and Henderson, 2013]. Erbe et al. (2012 and 2014) demonstrated the potential for applied value of sound maps by modelling shipping sound in Canada's Pacific Region and combining the acoustic distribution with density estimates for marine mammals that are of conservation concern [Borja et al, 2010]. However, the applied value of sound mapping and comparisons among sound sources relies on adequate acoustic processing and propagation formulas that vary per sound source type and environmental conditions such as water depth.

In the present section, we provide a case study that elucidates the state of the art and the potential for applications of marine sound maps worldwide. Sound maps are calculated for the shallow water environment of the Dutch Exclusive Economic Zone (henceforth abbreviated "Dutch North Sea"). This part of the North Sea is a heavily exploited area providing vessel entrance to the largest port in Europe (Rotterdam), and other activities adding to underwater acoustic load include: fisheries, several busy ferry lines between England and the Netherlands, the operation and construction of wind farms, seismic surveys and detonation of unexploded World War II ordnance. We here investigated the spatial, temporal (weekly) and spectral distribution (averaged over two years) of energy with a hybrid method [See sections 2.2 and 2.3], which enables the fast calculation of propagation loss across a wide range of frequencies. Because energy adds linearly, this approach permits the calculation of a sound energy budget per source. In this study, realistic source distributions are used to generate sound maps for each source and for the energy sum (incoherently) of all sources. Energy contributions of each sources are analysed for a wide frequency band 100 Hz to 100 kHz. The water depth in the Dutch part of the North Sea is mostly less than 50 m. This shallow water environment hosts various geophysical, biological and anthropogenic sources. Geophysical sources include wind, rain and lightning and can be prominent. Biological sources include communication and feeding sounds from invertebrates, crustaceans, fish and marine mammals, but are not thought to contribute significantly to the overall sound energy budget in the North Sea [Ainslie et al, 2009].

The purpose of our sound maps is to provide insight into the relative contribution of sound sources to the overall cumulative distribution of sound energy in space, time and spectrum. This will allow evaluation of potential environmental impact on different animal species living in the Dutch North Sea. The potential impact will vary per species depending on species-specific geographic distributions, the (seasonal) timing of critical activities and the absolute and spectral sensitivity to sound. Providing sound maps must be seen as a starting point for impact assessment and possible mitigation, as consequences of sound exposure are typically still unclear and there are more factors than source and propagation characteristics that will affect the sound exposure levels in marine animals. Pinnipeds are for example particularly common around the Wadden islands in the north, while many fish spawn in the southern part of the North Sea. The harbour porpoise is known to exhibit large fluctuations in density among different months of the year and some diving birds are present year-round, while others are only present in winter. Furthermore, the spectral range of auditory sensitivity varies per taxonomic group and can be broadly categorized: invertebrates (most likely < 300 Hz, some up to 3000 Hz) and fish (many < 500 Hz, most < 1000 Hz, all < 4000 Hz) and marine mammals: seals (0.3-60 kHz) and porpoises (1-125 kHz).

The starting point for constructing sound maps is the assessment of the acoustic energy generated by various sources. [Ainslie et al., 2009] introduced the concept of the “free-field energy” of a sound source, defined as the total acoustic energy that would exist in the water if the same source were placed in an infinitely deep ocean, of uniform impedance, no boundaries other than the sea surface, and with the same sound speed, density and absorption coefficient as seawater. This quantity is proportional to the source power and inversely proportional to the absorption coefficient of seawater, and provides a convenient way of ranking the contribution to the sound field from qualitatively different natural and anthropogenic sources. By adding the contributions from individual sources [Ainslie et al, 2009] made order of magnitude estimates of the contributions of different sound sources to the annually averaged free-field energy. We here follow up with more precise calculations and more extensive visualizations of variation in space, time and spectrum for the sound energy distribution in a real-world case study for the Dutch North Sea.

We calculate and compare the total energy contributions from four sound sources taking into account the environmental conditions in the Dutch North Sea. We do so by characterizing the spatial, temporal and spectral distributions of sound using previously developed source models [Weston 1960; Wales and Heitmeyer,2002; Sertlek and Ainslie,2015a; Kuperman and Ferla,1985; APL-UW,1994; Ainslie 2010; Arveson and Vendittis,2000] and propagation models [Ainslie et al

2011; see Section 2.3]. We included three anthropogenic sources: ships, airguns and explosions, and one geophysical source: wind. While sophisticated pile driver source models exist [Reinhall and Dahl 2011; Zampolli et al 2013], the coupling of such source models with accurate propagation models is an active research topic in its own right [Schecklman et al 2015; Lippert et al,2015; Hall,2015] and is beyond the present scope. We have chosen to focus on wind as our geophysical sound source because of its ubiquitous nature, while rain and lightning can also contribute significantly to the acoustic energy budget.

The aims of the present section are:

- to quantify the contributions from ships, airguns, explosions and wind to the overall acoustic energy in the Dutch North Sea;
- to develop and apply quantification methods for providing insight into the spatial, temporal and spectral distribution of that energy;
- to provide an evaluation of the potential biological relevance.

In Section 3.4.2, we describe the inputs needed to generate the sound maps (source levels, bathymetry, sediment properties) and propagation method. In Section 3.4.3, two-year average sound maps are presented for the Dutch North Sea. We provide histograms and cumulative distribution functions derived from the spatial distribution of SPL (the squared sound pressure is averaged over two years), followed by the temporal distribution of sound energy contribution from each source in Section 3.4.4. In the final section, the proposed approach and results are summarized and discussed in the context of biological relevance and as a tool for policy makers, offshore industry, and conservationists.

3.4.2. TOWARDS SOUND MAPS

A. Source Level

We examined three anthropogenic sources (ships, seismic airguns and explosions) and one natural source (wind). These sound sources have a variety of different sound generation mechanisms. It is conventional to characterize underwater sound sources in terms of their "source level". Unfortunately, this term has multiple different meanings, depending for example on the continuous [Wales and Heitmeyer,2002] or impulsive [MacGillivray,2006] nature of the source, or its proximity to the sea surface, whereby some sources are characterised in terms of the properties of the dipole formed in combination with their surface-reflected image, [Ziolowski,1970; Arveson and Vendittis,2000], while others are treated as a monopole regardless of their position relative to

the sea surface [Weston,1960; Wales and Heitmeyer,2002]. Finally, some sources, like wind and rain are more naturally described as sheet sources than as point sources. These multiple differences make it difficult to make meaningful comparisons between the source levels of different types of sources. Since each source has a different sound generation mechanism, there are different frequency-dependent patterns of amplitude fluctuations (Figure 1). Consequently, the comparison between any pair of sources is facilitated by first converting them to a common metric (as described in Appendix A).

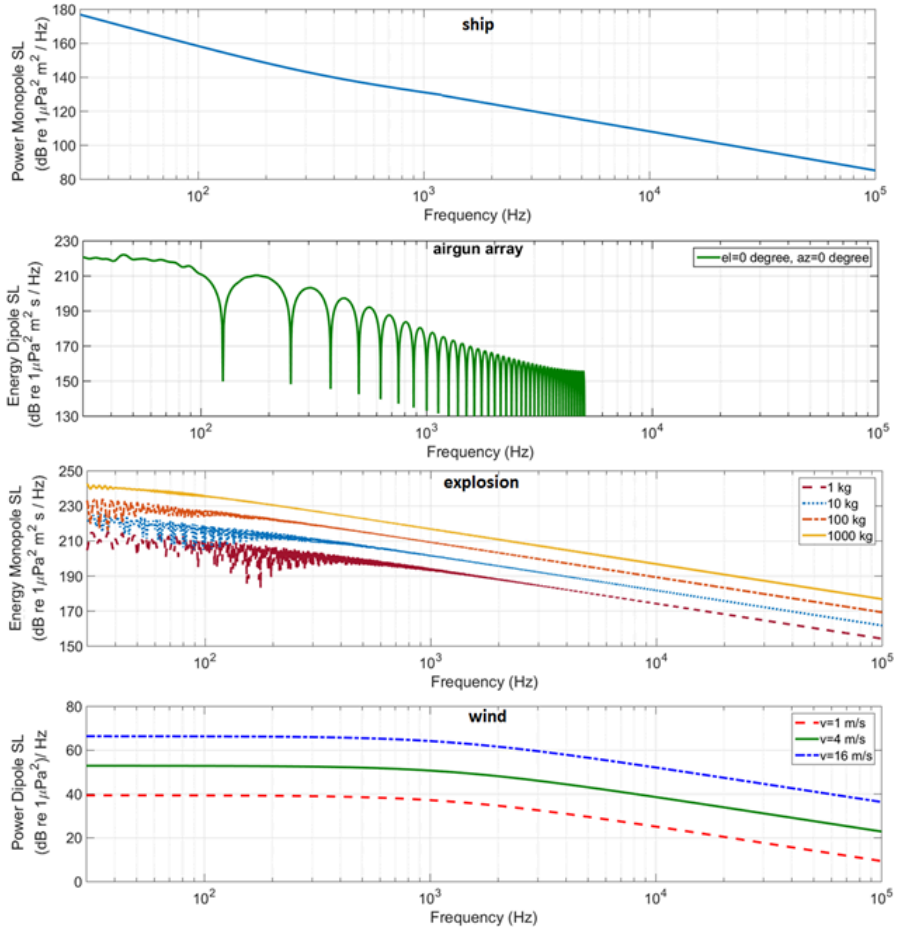

*Figure 1. Spectral density source level for a monopole source of ship (extrapolated Wales and Heitmeyer formula) at 5 m source depth (*based on information from [Gray & Greeley, 1980] and [Arveson & Vendittis, 2000]*), for an energy dipole source level of an airgun array [Sertlek and Ainslie, 2015] at 6 m source depth, a monopole source of an explosion [Weston,1960],and an areic dipole spectral density level of wind (merged [Kuperman and Ferla,1985] and [APL-UW,1994] models)*

For ships, the source level is often characterised in terms of the radiated sound level [ISO 17208-1, Arveson and Vendittis]. The dipole source level description of ships is also possible although it is rarely used. We used the measurements of Wales and Heitmeyer, who measured the average *monopole* source level of different ships at different speeds [Wales and Heitmeyer,2002]. Their formula has been used here, extrapolated to high frequencies according to [Ainslie,2010 (p 423)]. An airgun operates by releasing a bubble of air under high pressure from the gun chamber into water. This creates a high pressure spherical pulse in the water that travels away from the bubble and is subsequently reflected from the sea surface.The oscillating bubble pulses are the main modulator of the spectrum. On the other hand, the interference between the airgun pulse and its surface reflection causes the oscillations in its energy source level. Depending on the positions of the airguns in the array, energy source level varies with elevation and azimuth angles. A numerical procedure has been used to quantify the airgun source signature based on bubble dynamics, mass and heat transfer and validated for frequencies up to 1 kHz [Sertlek and Ainslie,2015]. At higher frequencies, more advanced techniques are required to model nonlinear interactions between the bubbles. Consequently, we plotted the energy source level in Fig. 1 up to 5 kHz. The vertical variation in energy dipole source spectral density level for an airgun array is shown in Fig. 2.

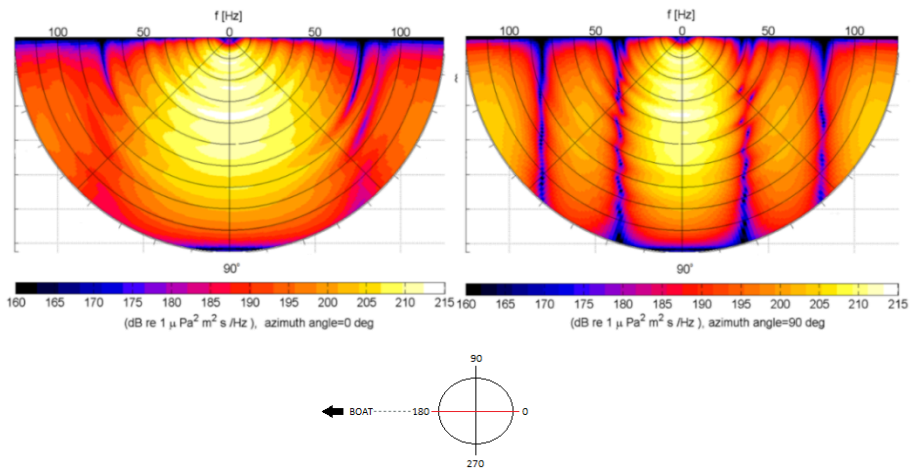

Figure 2. Vertical variation of energy dipole source spectral density level vs elevation angle (angle from the horizontal direction) of airgun array at azimuth angle=0 degree (left) and azimuth angle=90 degree (right). The source depth is 6 m.

The waveform resulting from an underwater explosion consists of a rapidly rising and decaying shock wave followed by a series of bubble pulses [Cole, 1965]. The interference between the shock

wave and bubble pulses results in the oscillations seen in Figure 1, especially at low frequency. For the acoustical characterisation of explosions, we adopted Weston's empirical formula [Weston,1960], which treats the explosion as a monopole source, without surface interaction. We convert Weston's characterisation to an equivalent monopole source level by assuming linear propagation from a distance of 5000 charge radii [Von Benda-Beckmann et al, 2014]. Von Benda-Beckmann et al, 2015] describes the uncertainty in the predictions of the energy source level of explosions in the shallow water and introduces a correction term which is based on the measurements. According to their paper, it was found that the use of the Weston/Cole formula for source level overestimates the sound exposure level , suggesting that the energy source level should be reduced by this amount to compensate. This correction term is added to results to increase the accuracy of calculated results in this paper. For the frequencies above 10 kHz, a flat variation of this correction factor is assumed (after a personal communication with Von Benda-Beckmann).

The variation of sea state or wind speed affects the source level of wind. Because wind produces sound over the entire sea surface, wind is usually characterized as a dipole sheet source [Kuperman and Ferla,1985; APL-UW,1994; Ainslie 2010], with the source level associated with a unit area of an infinite plane sheet. The properties of the four types of sources are described in turn, and summarised in Table 1.

Table 1. Source characteristics for the selected sources. The meaning of "source level" is different for each type of the sources.

Source	**Quantity**	**ISO/DIS 18405**	**Temporal Pattern**
ship	power monopole SL	source level(1)	Continuous
airgun	energy dipole SL	surface-affected energy source level(2)	Impulsive
explosion	energy monopole SL	energy source level(3)	Impulsive
wind	power dipole SL (areic)	surface-affected areic source level(4)	Continuous

(1)level of the source factor, (2)level of the surface-affected energy source factor, (3) level of the energy source factor and (4)level of the surface-affected areic source factor

B. Spatial and temporal Distribution of sources in the Dutch North Sea

Our aim is to gain insights in the distribution of sound across the Dutch North Sea, and to achieve this goal we analyzed the spatial, temporal and spectral distribution from various sources over a nominal two-year period. Due to limitations in availability of source data it has not been possible to select the same two-year period for all sources. Instead we constructed a fictional two-year period by combining the years 2007-2008 (seismic surveys [www.nlog.nl]) with 2010-2011 (explosions [KNMI] and wind [KNMI]) and 2013-2014 (shipping [www.marinetraffic.com]), (for shipping we have data for 2014 only, and these data are assumed representative for 2013 also). The resulting distributions of shipping, seismic surveys, explosions and wind speed are shown in Figure 3. The spatial distribution and timing of especially seismic surveys, and to a lesser extent explosions, will vary per year and depend on the particular localities and time periods of specific activities (more occurrence information can be found at the seismic survey data portal (see www.nlog.nl).

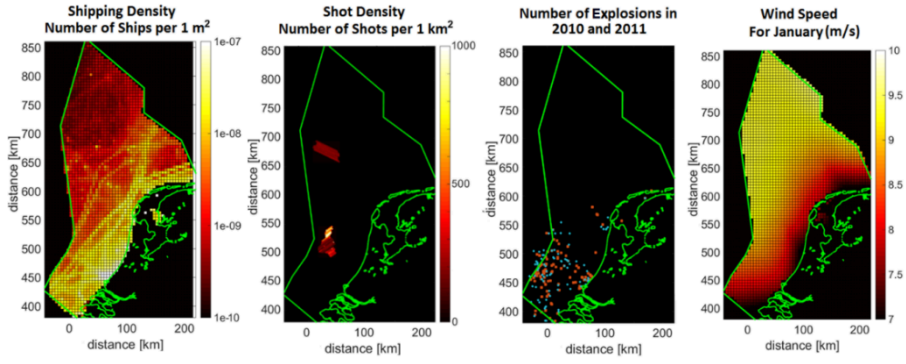

Figure 3.The distribution of areic shipping density (Number of ships per square kilometer) (left), seismic surveys (number of shots per square kilometer for 2007) (middle left), location of individual explosions between 2010 and 2011 (middle right) and Wind speed (m/s) for January (measured at 10 m above sea surface and extrapolated to the Dutch North Sea (right). Maps are based on the RD (Rijksdriehoek) coordinates [https://nl.wikipedia.org/wiki/Rijksdriehoekscoordinaten]

Shipping density maps and airgun array shot density maps were calculated for 5 km x 5 km resolution. The source factor [described in Appendix A; Ainslie 2010; ISO/DIS 2015] was multiplied

by the number of ships or shots (by taking into account the directivity effects) in each source grid. The calculated notional signatures (far-field signatures of individual airguns, without the surface reflection) were coupled with a propagation model to estimate the horizontal and vertical directivity pattern [Eq.(4) from MacGillivray, 2012].

C. Environment : Spatial distribution of water depth and sediment properties

The underwater propagation of sound depends on various geophysical factors such as water depth and sediment type. The bathymetry and sediment grain size maps for the Dutch North Sea are shown in Figure 4. For the bathymetry, the EMOD-NET database is used [Emodnet, 2014]. The sediment maps are provided by the Geological Survey of the Netherlands project [http://www.en.geologicalsurvey.nl/.]. Sediment data were not available outside the Dutch North Sea. These data are only required for the explosion maps, which include explosions outside the boundaries of the Dutch North Sea. For this case, it is assumed to consist of 'medium sand' [North Sea Atlas]. The sea surface is modelled as a flat pressure release surface (pi phase change in radians). The acoustic medium is assumed as two layered waveguide by neglecting the effects of sub-bottom material (even though this might be significant for the low frequency sound). The geoacoustic properties of the seabed material are inferred from the grain size using Table 4.17 of Ainslie 2010. The isovelocity approximation, which does not lead to large errors in the shallow water environment of the Dutch North Sea, is used [See Section 3.1]. Urick's equation for volume absorption [Urick 1976, second edition; Fisher and Simmons,1977] is used, which includes the boric acid relaxation at low frequency [See Appendix A].

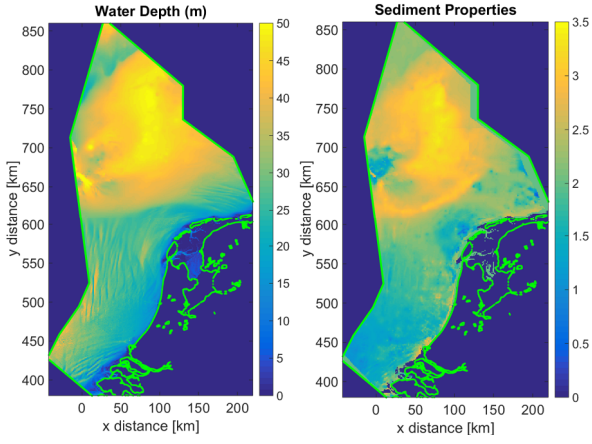

Figure 4. Bathymetry (water depth, in metres) (left) and sediment grain size (-log$_2$(Grain diameter/(1 mm))) (right) maps of the Dutch North Sea.

D. Underwater sound propagation

While [Erbe et al. 2012 and 2014] illustrate the potential application for sound maps in localizing acoustic conflicts at ecological hot spots, their sound propagation modelling approach leaves room for improvement. First they approximate the dipole source created by the ship and its surface image at low frequency with a monopole with the same power as the dipole (personal communication C. Erbe, 11 February 2016) Second, they assume the cylindrical spreading region extends indefinitely far from the source, which for a line source leads to an unphysical situation in which the sound pressure level becomes independent of distance from the source, a form of Olbers' paradox [Olbers, 1826]. An improved approximation could be obtained, with no extra effort, by applying the simple geometric spreading rules described by [Ainslie et al, 2014], comprising a modified cylindrical spreading region ($10 \log 10\ R$) followed by a mode stripping region characterised by $25 \log 10\ R$ [Denham, 1986] for a dipole source instead of the usual $15 \log 10\ R$ for a monopole [Weston 1976].

In the current section, to simulate the propagation problem efficiently, we used a hybrid propagation model (called "SOPRANO") based on normal mode and flux theories [Sections 2.2 and 2.3]. The accuracy of this propagation model was investigated with multi-model comparisons [Sections 2.2 and 2.3]. SOPRANO can calculate the PL for a variable sediment type and bathymetry with an accuracy similar to the adiabatic mode theory (The differences between Soprano and KrakenC (adiabatic approximation) are less than 0.2 dB for the selected test cases in Section 2.3. The maximum difference is less than 2 dB for the realistic Dutch North Sea bathymetry (not shown).

PL is calculated over radial slices with 1 degree resolution. For ranges up to 1 km, small range steps are used (25 m). For longer ranges, PL is calculated for each 250 m intervals. Mean-square sound pressure (p_{kn}^2) is also spatially averaged over all receiver cells for the kth receiver depth as

$$p_{ijk}^2 = \frac{\sum_{n=1}^{N_{SPL}} r_n dr_n p_{kn}^2}{\sum_{n=1}^{N_{SPL}} r_n dr_n}$$

where dr_n is the range steps and N_{SPL} is the number of the discrete point in the receiver cell. Then, mean square sound pressure at each receiver cell (p_{ijk}^2) is averaged over receiver depths in order to take into account the variability of PL at the different receiver depths as

$$p_{ij}^2 = \frac{\sum_{k=1}^{K} p_{ijk}^2}{K}$$

where K=10 receiver depths which are equally spaced from 1 m below the sea surface to 1 m above the seabed.

For natural sources, the approximations used are slightly different than the modelling approach of anthropogenic sound sources. Wind sound sources are described as a sheet dipole source [Kuperman and Ferla,1985; APL-UW,1994; Ainslie,2010]. The contribution from wind is calculated by an analytical approach [Ainslie et al, 2011], assuming a flat seabed. Thus, the calculations are done separately for each 5 km x 5 km grid cell by assuming a constant water depth in these source cells.

3.4.3. SOUND MAPS OF THE DUTCH NORTH SEA

Spatial, temporal and spectral analysis of the sound field

In this section, sound maps of the Dutch North Sea are shown (in Figure 6), with attention to the spatial distribution of SPL and the temporal distribution of total sound energy from the four selected sources, as well as for all sources together (all based on two-year averages). We seek a measure of sound with which we can make a like with like comparison between qualitatively very different sources (ships, airguns, explosives and wind). We wish to compare, for example, impulsive sounds with continuous ones, and sheet-like sources with point-like sources. One way of achieving this in principle is to look at their impact: how many animals are affected and in what way? In practice this would be a huge undertaking, partly because so little is known about the effects of underwater sound on most species, and partly because, even for the species for which such knowledge is partly available, it would require a multi-disciplinary activity involving acousticians, physiologists and ecologists that is beyond the scope of the present work. An exception is made for the case of an explosion [See Chapter 4], for which the impact is assessed by each explosion using SEL for that explosion, and then the cumulative impact for all explosions in a two-year time period is estimated. It is reasonable to assume that the effect increases with SEL per explosion and with the number of explosions. A natural physical measure that incorporates both is the total sound exposure accumulated over (say) a year, a quantity that is closely related to the

total energy, averaged over a year. While not a direct measure of impact, it is a useful metric that one can calculate for all 4 sources, and for which one can assert with some confidence that the risk associated with any one source will increase with increasing (annually averaged) energy [Ainslie & Dekeling 2011].

Visualizations for both spatial and temporal variation in energy distribution are provided for different frequency ranges: the 125 Hz deci-decade band and three single-decade bands 100 Hz to 1 kHz (referred to henceforth as the 'low frequency', or 'LF' band), 1 kHz to 10 kHz ('mid-frequency', or 'MF' band) and 10 kHz to 100 kHz ('high frequency', or 'HF' band). (A deci-decade is a logarithmic frequency interval equal to one tenth of a decade [ISO/DIS 18405]. This frequency interval is sometimes referred to as a "one-third octave" because it is approximately equal to one third of an octave). The EU's MSFD requires its member states to monitor ambient sound in decidecade bands centred at 63 Hz and 125 Hz, the latter frequency being within the LF band considered in the present study. In the Dutch North Sea, average water depth is around 40 m-50 m, and 125 Hz sound is sufficiently above the cut-off frequency for the application of our propagation model. The frequency of 63 Hz is not included because as it is less than our minimum frequency (100 Hz).

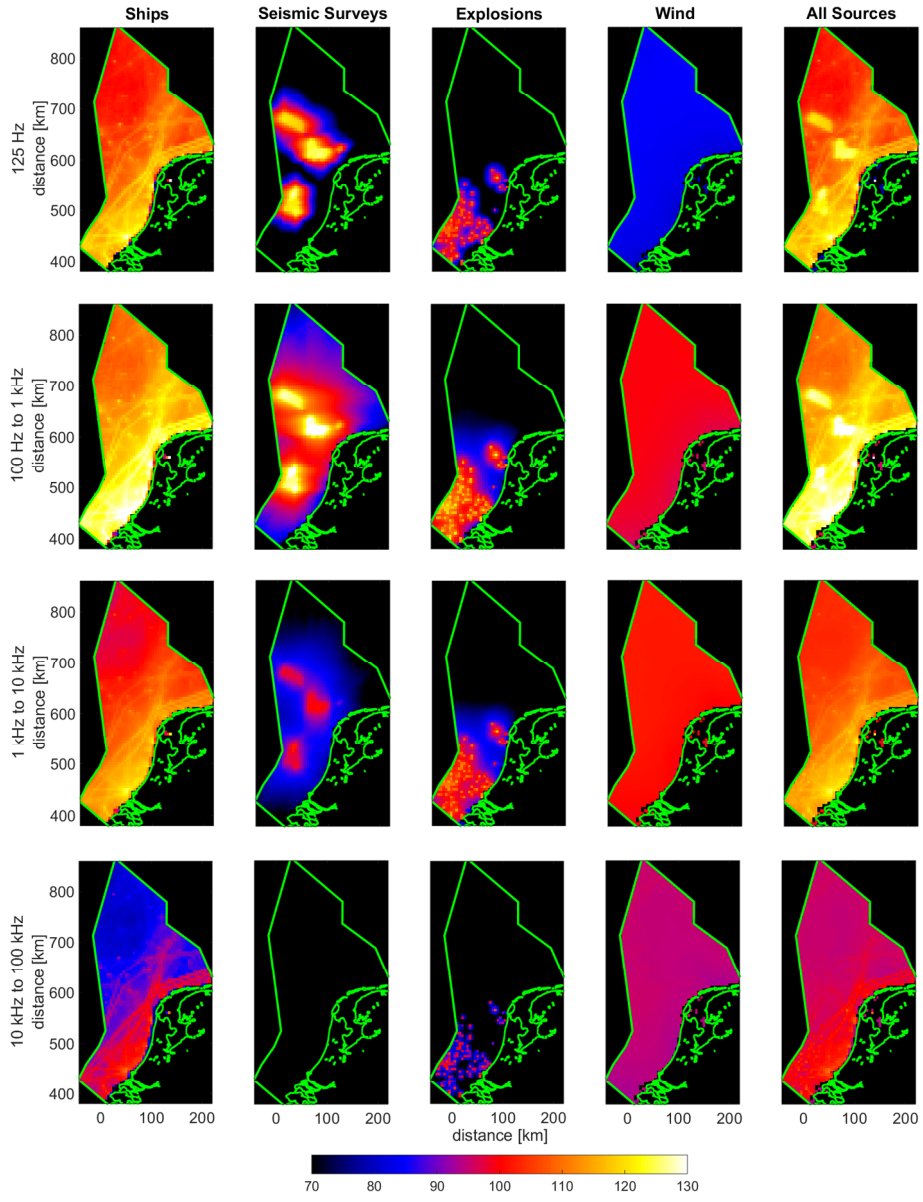

Figure 6. Two year average sound maps (SPL) for shipping, seismic survey, explosions, wind and sum of four sources. Squared sound pressure is averaged over receiver depth. The maps are generated for the 125 Hz decidecade frequency band, LF (100 Hz to 1 kHz), MF (1 kHz to 10 kHz) and HF (10 kHz to 100 kHz). The RD (Rijks-Driehoek) coordinate system used for the presented sound maps.

In Figure 7, we depicted spatial and temporal distribution of SPL (versus area) for LF, MF and HF bands. This histograms reflect the occurance distrubition of SPL over the Dutch North Sea. This figure provides a tool to assess the areas affected by different exceedance levels.

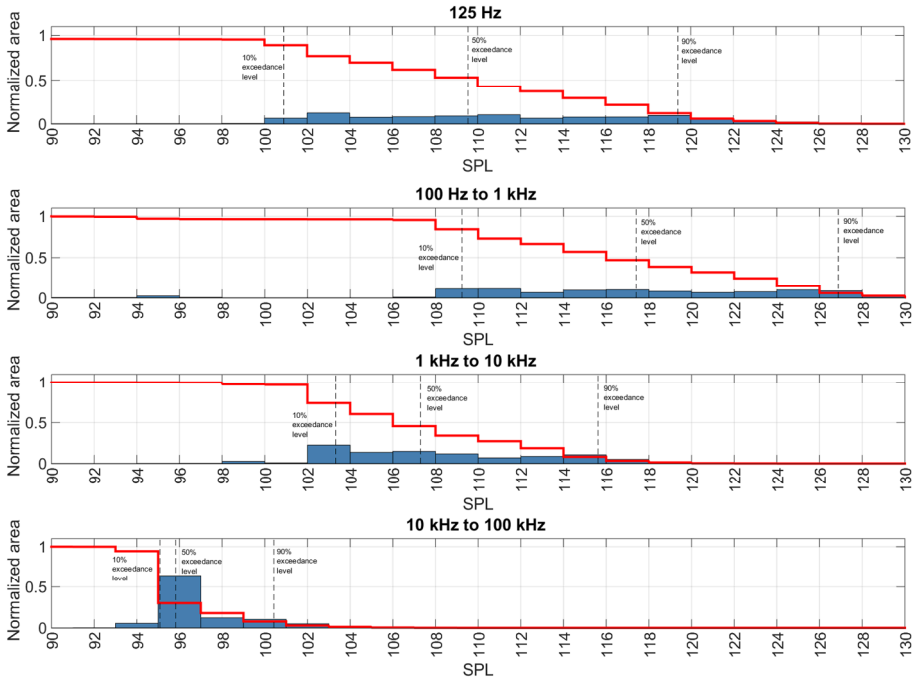

Figure 7. Histogram (blue bars) and cumulative distribution function(red lines) derived from the spatial distribution of the two-yearly averaged SPL for LF, MF, HF decade and 125 Hz decidecade bands in the Dutch North Sea. The area is divided by the total area of the Dutch North Sea (Normalized area). The 90%, 50% and 10% exceedance levels are indicated for each frequency band.

3.4.4. TEMPORAL AND SPECTRAL DISTRIBUTION OF SOUND ENERGY

Sound prediction tools can be used to estimate the contribution to the sound energy from each source. The benefit of quantifying contributions in terms of their energy is that the contributions can be added in a linear manner, making it possible to construct an energy-based sound budget. The total acoustic energy in the Dutch North Sea is calculated from spatial averages of the squared sound pressure which is based on the SPL sound maps in Figure 6 in order to understand what the

contribution is from each source to the total energy budget. The acoustic energies in the Dutch part of the North Sea are calculated at decidecade center frequencies by the following formula

$$E_{Total} = \frac{1}{\rho c_w^2} \int p^2(f, x, y, z) dV$$

This formula is approximated as

$$E_{Total} \approx \frac{1}{\rho c_w^2} \sum_{i=1}^{N_x} \sum_{j=1}^{N_y} p_{ij}^2 \, H_{ij} \, \Delta x \, \Delta y$$

where $\Delta x \, \Delta y$ are the dimensions of the receiver grid (the resolution of sound map), N_x and N_y are the number of receiver cells in x and y directions, H_{ij} is the water depth of the receiver cell, ρ is the density of the sea water, c_w is the sound speed in the water column and p_{ref} is the reference pressure.

The energy contributions from each source to the total acoustic energy are plotted in Fig. 8. The number of shots and the size of the weekly covered area by seismic surveys are estimated from the seismic survey reports. Then, the sound maps are scaled by this ratio. Figure 8 shows that shipping makes a dominant contribution in most weeks, with sporadic interruptions from explosions (e.g., week 8 for HF) and airgun surveys (e.g., week 51 for the 125 decidecade band and LF). Wind makes the largest contribution for HF.

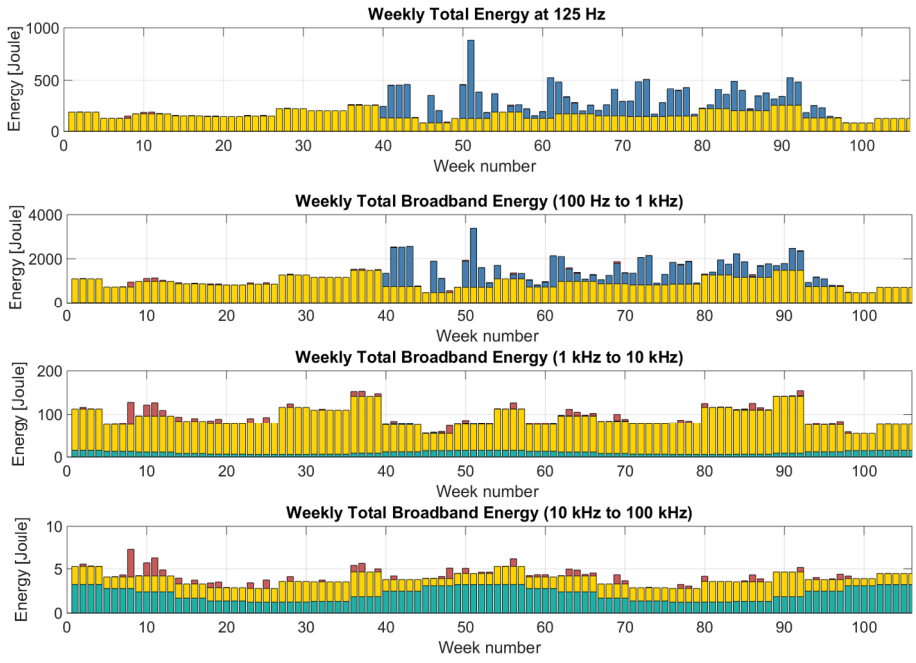

Figure 8. Weekly averaged total acoustic energy (in joules) vs time in LF, MF, HF decade bands and the 125 Hz decidecade band. The week numbers show time in weeks from 1 January of the first year

In any one week, activitities of relatively short duration such as seismic surveys and (especially) explosions can make a larger contribution than shipping. For example, the explosions make a larger contribution than shipping in the 8th, 9th and 11th weeks in the HF band. The seismic surveys make a larger contribution than shipping in the 51st week as shown in Figure 8 in the LF band. The effect of averaging time for SPL is investigated in Appendix B.

Figure 9 shows the spectral distribution of two year averages of total energy in decidecade frequency bands. Having calculated the contibution to the total sound energy from each type of source it was also possible to construct an energy budget, showing the proportion of the total for each. These comparisons for the total acoustic energy provide insight into the ranking of the sources according to their contributions to the total acoustic energy during the two year time period. At the low and medium frequency band (LF and MF), shipping activities have the largest contributions (920 J and 80 J). For the mid-frequency range, the contribution from wind increases, and dominates the energy budget at frequencies exceeding 5 kHz (2 J for HF). For HF, the energies of shipping and explosions are very similar (about 0.2 J). The contribution from seismic surveys is very low above 1 kHz.

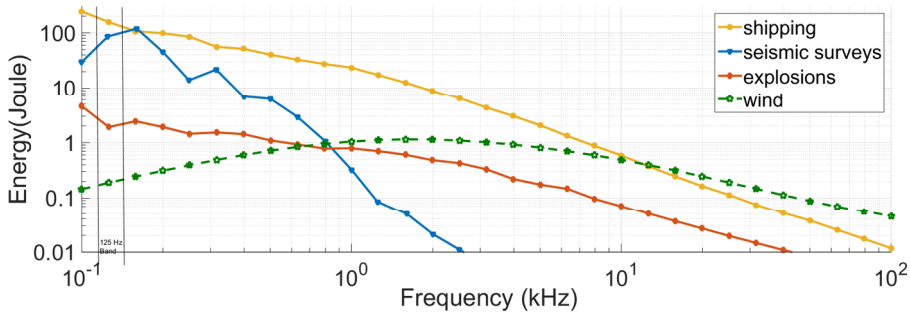

Figure 9. Two year average of total acoustic energy in the Dutch North Sea, in deci-decade bands.The shipping is making the largest contribution up to 5 kHz. Wind is the largest contributor above 5 kHz. The seismic surveys are contributing at the low frequencies (up to 1kHz).

The relative energy budgets for the different sound sources are summarised in Table 2 for the various frequency bands (125 Hz, LF, MF and HF). This table is based on the long-term average (2 years) of the acoustic energy. The energy averaged over two years for 100 Hz to 100 kHz band is 1346 J, of which 72.8 % is from shipping, 24.4 % from seismic surveys and 1.6 % from explosions. The estimated contribution from wind is 1.2 %. The mean SPL is dB re 1 uPa^2 for 100 Hz to 100 kHz band. The total energy for 125 Hz band is 243 J, of which 64.3 % is from shipping, 34.8 % from seismic surveys and 0.8 % from explosions. The estimated contribution from wind is 0.1 %. The mean SPL is 114.2 dB re 1 uPa^2 for 125 Hz band.)

Table 2.The average sound energies for 125 Hz decidecade, and LF, MF and HF decade bands.

	Average sound energy in the Dutch North Sea				
	125 Hz decidecade	**LF decade**	**MF decade**	**HF decade**	**100 Hz to 100 kHz**
shipping	160 J	920 J	80 J	2 J	980 J
seismic surveys	85 J	330 J	0.4 J	-	330 J
explosions	2 J	19 J	4 J	0.25 J	22 J
wind	0.2 J	6 J	10 J	2 J	17 J

In Appendix A, the free-field energy associated with ships (3900 kJ), airguns (1000 kJ), explosions (110 kJ) and wind (15 kJ) are calculated for the same two-year period and for the same frequency band (100 Hz to 100 kHz) as the total sound energy in Table 2. It is expected to see larger energies in the free field because of the shallow water propagation leading to loss of energy into the seabed. This effect is especially pronounced for dipole-like sources (ships, airguns, wind), which direct their sound energy preferentially towards the seabed.

3.4.5. BIOLOGICAL RELEVANCE

The sound maps (shown in Figure 6) , the information on spatial variation (Figure 7) and the energy distributions (Figure 8 and 9) can all be used for biological impact studies for different fish and marine mammal species [MacGillivray 2006; Erbe et al 2012 and 2014; Bouton et al, 2015]. The relationship between the frequency band categories and animal hearing ranges is depicted in Figure 10. Fish are sensitive to the low-end of the spectrum, while marine mammals are sensitive to broad ranges, with baleen whales going very low and overlapping with fishes, toothed whales and dolphins going very high into the ultrasonic, and pinnipeds somewhere in between.

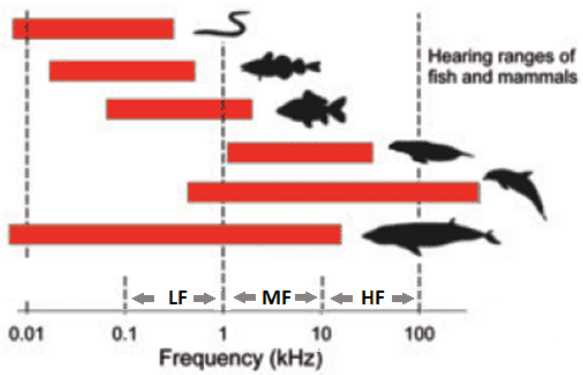

Figure 10. The hearing ranges of fish and mammals in LF, MF and HF bands (adapted from Slabbekoorn et al,2010)

The geographical distribution of sound energy conveyed by the sound maps can provide information of relevance to the ecology of the Dutch North Sea by comparing this distribution with that of local marine life [CetSound, Sutton et al, 2011 ; Porter and Henderson, 2013]. After

combining Figure 7 with animal density maps or species-specific habitat-quality maps, one can add species specific disturbance thresholds to estimate how many animals or how badly a specific species is affected in the Dutch North Sea. For example, the CetSound Project investigates cetecean distribution in U.S. Exclusive Economic Zone (EEZ) and develops regional sound maps for low frequencies(50 Hz to 1 kHz) for multiple sources. The merger of these cetecean density and sound maps gives insight into the impact of sound on the animal distribution for different regions (for Beaufort and Chukchi Seas, Gulf of Mexico and Atlantic Coast). Similar studies are also done to investigate the impact of the underwater explosions on the distribution of harbour porpoises in the Dutch North Sea [see Sections 4.1 and 4.2].

The temporal distribution of sound is also relevant, but the current temporal resolution that we used (one week) seems unlikely to be sufficient to make meaningful statements in this regard, because it is expected that animals respond to sound on a shorter timescale (order of seconds, minutes or hours, rather than weeks). For this reason, the averaging time of sound maps is critical for the transients. Appendix B shows the impact of using different averaging times for assessing the SPL. The smaller the averaging time the higher the maximum SPL and the higher the spread in the temporal distribution. The impact assessment studies for each individual event will thus require a careful choice of the averaging time [Madsen,2005; Sertlek et al, 2012]. Long averaging times lead to stable averages that make the results more comparable for different sources. The EU Noise expert group TSG Noise therefore recommends annually averaged sound maps for management purposes [Dekeling et al 2014], but it should be clear that assessing the biological impact of the various sources on specific communities or species requires to take the temporal dimension into account. Furthermore, it is important to realize that there are still a lot of uncertainties when it comes to acoustic thresholds for hearing across species and also little is known about impact of audible sounds on free-ranging animals in terms of individual fitness and population consequences [Popper et al. 2004; Slabbekoorn et al. 2010; Radford et al. 2014]. Sound maps may be helpful in guiding future research efforts towards most critical species or most critical areas as well as in site selection for sampling designs.

3.4.6. SUMMARY AND CONCLUSIONS

Our study aims to provide a calculation strategy for shallow water sound maps, which can be a useful tool for assessing the risks associated with anthropogenic sounds in the marine environment. This is achieved by developing a fast and accurate shallow water broadband

propagation method which enables the calculation of the results for a wide range of frequencies. The sound map analyses of the Dutch North Sea, based on realistic sound source levels and real events, revealed that most sound energy comes from ships, followed by airguns and explosions, with most energy at frequencies between 100 Hz and 1 kHz for all three anthropogenic sources. It should be noted, however, that this ranking is likely to vary from year to year depending on the agenda of human activities and will also be different for other marine areas. We therefore stress that our main message is not in the absolute values or specific source rankings or sound distribution details. We believe the main value of this work is the mapping approach using source specific and propagation-conditions dependent algorithms. Also interesting for extrapolation to other years or other areas is that all anthropogenic sources exhibited strong geographical signatures despite the relatively small scale of our case study.

The call from society for more information about the distribution and impact of sound levels underwater is growing, as we know sound is likely to play a dominant role in the life of many aquatic animals [Myrberg and Fuiman 2002; Montgomery et al. 2006; Slabbekoorn et al. 2010] and a variety of human activities add considerable amounts of sound to the naturally present levels. We typically do not know whether the elevation of sound levels undermines the “Good Environmental Status” of a particular waterbody [Dekeling et al 2014], but potential impact includes masking of critical sounds and other detrimental effects of distraction, disturbance, deterrence and injury [Popper and Hastings 2009; Slabbekoorn et al. 2010; Radford et al. 2014]. International concern about these possible effects has already found its way into regulatory measures worldwide [Lucke et al. 2014] and we believe our mapping methodology provides a useful toolbox for example to meet specific monitoring requirements on particular frequency bands in the Marine Strategy Framework Directive (MSFD) of the European Union [EU 2008].

Our approach of generating integrative maps for multiple sources can also give insight into the contribution of specific sources to an overall soundscape (acoustic footprint) and allows exploration of potential impact of individual sources or cumulative effects on specific areas, communities or species. Therefore, while sound may or may not turn out to significantly affect marine life in different cases, the current state of the art in underwater sound mapping allows us at least to adequately depict and investigate the temporal and spatial distribution of anthropogenic sound in the context of natural fluctuations in ambient noise. We hope our work will stimulate future applications and guide further impact studies with appropriate data on underwater acoustics.

APPENDIX A- CALCULATION OF FREE FIELD ENERGY

In this appendix, the calculation of free field energy is described. The "free-field energy" of a sound source is calculated by following the approach from Ref [Ainslie et al 2009] . E_f is not the true acoustic energy associated with the source, but the energy that would exist in the sound field produced if the same source were placed in free space (an infinitely deep ocean, of uniform impedance, no boundaries other than the sea surface, and with the same sound speed, density and absorption coefficient as seawater) and operated at the same source level. The spectral density of the free-field energies E_f of these sources can be calculated from the average power W_f [Ainslie et al, 2009]

$$E_f = \frac{W_f}{2\alpha c_w}$$

where ρ_w is density of water, c_w is sound speed in water and α (Np/m) is the volume absorption coefficient.

Here, free field energy is proportional to the source power and inversely proportional to the absorption coefficient of seawater, and provides a convenient way of ranking the contribution to the sound field from qualitatively different natural and anthropogenic sources. The source power spectra tell us how much sound is radiated by monopole, dipole and sheet sources, but it falls short of a complete picture because the source power does not tell us how far the sound propagates, and in particular takes no account of the efficient propagation (low absorption) of sound at low frequency.

The first step towards a quantitative comparison of free field energies is to estimate the source power spectra and compare those. To summarise, the average power spectral density, added over all sources of a given type, is shown in Table A1.

Table A1. The source powers for ship, explosions, airguns and wind.

Source Type	W_f (Source Power)	Description
Ship	$W_f = \frac{2\pi}{\rho c} \sum_{i}^{Number of Sources} \int_{0}^{\pi/2} S_{f,i}^{\mathrm{dp}} \cos\theta \, \mathrm{d}\theta$	For the ships the surface-affected (dipole) source factor is $S_f^{dp} = S_f^{mp} \, 4 \sin^2 kz_s \sin\theta$. The total number of ships in the monthly averaged density maps for 2014 varies between 500 and 950.
Explosion	$W_f = \frac{1}{T}\frac{2\pi}{\rho c} \sum_{i}^{Number of Sources} \int_{-\pi/2}^{\pi/2} S_{E,f,i}^{\mathrm{mp}} \cos\theta \, \mathrm{d}\theta$	$S_{E,f,i}^{\mathrm{mp}} = (\rho c) r^2 E(\omega, r)$, $E(\omega, r)$ is the spectral density of the sound energy flux density (including the shock wave and the first two bubble pulses) and r is a distance beyond which the sound is assumed to behave linearly ($r \approx$5000*radius of the explosive) [Ainslie, 2010]. t is the averaging time. Total number of explosions are 232.
Airgun	$W_f = \frac{1}{T}\frac{1}{\rho c} \sum_{i}^{Number of Sources} \int_{0}^{2\pi} \int_{0}^{\pi/2} S_{E,f,i}^{\mathrm{dp}} \cos\theta \, \mathrm{d}\theta \mathrm{d}\phi$	$S_{E,f,i}^{\mathrm{dp}} = 2\lvert q(\mathrm{f}, \theta, \phi)\rvert^2$ and $q(\mathrm{f}, \theta, \phi)$ is the frequency domain source signature as described in [Sertlek, Ainslie,2015]. T is the averaging time.
Wind	$W_f = \frac{2\pi}{3\rho c} A K_f$	The areic source factor per unit area is described as [Ainslie et al, 2011] $\mathrm{K_f} = \frac{10^{4.12}\left(v/(1\ \mathrm{m/s})\right)^{2.24}}{1.5+\left(\frac{f}{1000\ \mathrm{Hz}}\right)^{1.59}} \mu\mathrm{Pa}^2/\mathrm{Hz}$. The annually averaged wind speed is calculated as $\left(\overline{(v)^{2.24}}\right)^{\frac{1}{2.24}}$ =6.78 m/s from 12 months of wind speed data measured at 10 m above sea surface in the Dutch North Sea [KNMI]. where A is the total area.

By using the free field energy formulation, the comparison in Figure A1 can be done. The free field energies of all explosions, ships and seismic surveys in two year time period are shown. The calculation of energy is very sensitive to choice of absorption formula at low frequencies. The

volume absorption is calculated by Thorp formula which includes the low frequency effects [Fisher and Simmons,1977]

$$\frac{\alpha}{Np/m} = \frac{10^{-3}}{20\log_{10} e}\left[\frac{0.1}{0.9144}\frac{(F)^2}{1+(F)^2} + \frac{40}{0.9144}\frac{(F)^2}{4100^{0.5}+(F)^2} + \frac{2.7510^{-4}}{0.9144}(F)^2\right]$$

where $F = \frac{f}{1000\ Hz}$.

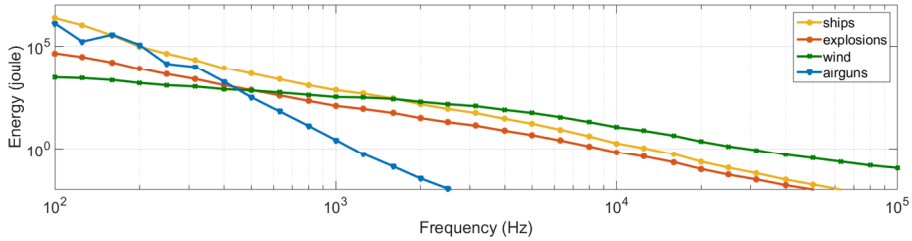

Figure A1. Total free field energies in decidecade bands of different sources averaged over year and Dutch North Sea. Source power is calculated for the total number of sources included. Although the source level cannot be directly compared, free-field energies (and source powers) can be compared between sources.

Table A2. Ranking of the sources for average radiated power per unit area and free-field energy. The source power is divided by the total area of Dutch North Sea (63687 km2)

Source Type	average power per unit area		average free-field energy	
	125 Hz decidecade band	broadband (100 Hz to 100 kHz)	125 Hz decidecade band	broadband (100 Hz to 100 kHz)
shipping	10.6 $\mathrm{nW/m^2}$	39.8 $\mathrm{nW/m^2}$	1060 kJ	3920 kJ
seismic surveys	0.85 $\mathrm{nW/m^2}$	10.1 $\mathrm{nW/m^2}$	169 kJ	1960 kJ
explosions	0.3 $\mathrm{nW/m^2}$	1.88 $\mathrm{nW/m^2}$	18.8 kJ	107 kJ
wind	0.03 $\mathrm{nW/m^2}$	2.26 $\mathrm{nW/m^2}$	2.60 kJ	15.2 kJ

Appendix B- THE EFFECT OF AVERAGING TIME

The choice of averaging time is critical, especially for transient sounds [Madsen,2005]. In the main section, we focus on long term (two years) and weekly averaged quantities. However, some of the biological problems related with the sound maps may need higher time resolutions such as a day, hour or second. The shipping and wind are ubiquitous sources, the sound of which is present throughout the year. By contrast, the sounds from explosions and seismic surveys are focused in time over a period of a few weeks (seismic surveys) or seconds (explosions). For instance, for the weekly averaged sound maps, the contribution from each explosion during the time the sound takes to spread away from the source immediately after an explosion would be about 10log10(1 week/100 s) dB, i.e., 38 dB higher than the levels shown in this section. A sound map of a single explosion, averaged over various time windows as 1 minute, 1 hour, 1 day, 1 week, 1 month and 1 year is compared in Figure A2 with the shipping sound map for January 2014. The purpose of this comparison is to demonstrate that the root mean squared (rms) sound pressure caused by the explosion, when averaged over a sufficiently short time window, exceeds that due to shipping over a large area. While the (monthly averaged) shipping sound map for January is not strictly comparable with the averages over durations of an hour or less, it provides a useful indication for the expectation value. It is immediately clear that when averaged over a short time window, the transient intensity exceeds that of continuous shipping over a large area, even in the presence of a high shipping density.

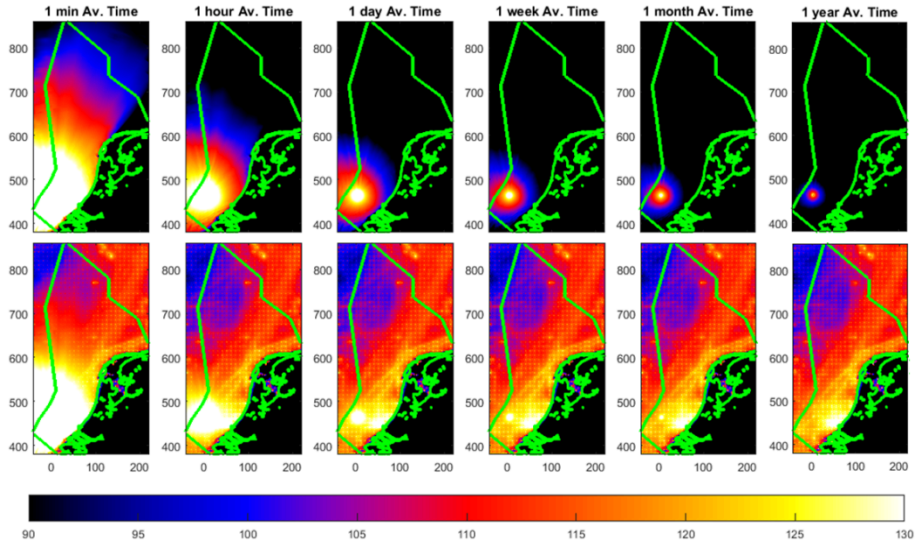

Figure A2. The effect of averaging time window is illustrated. In the upper maps, SPL maps of single explosion for the various time windows are shown. In the lower maps, these maps are summed with the shipping sound maps of January 2014.

Although we are aiming to find out what is the average contributions of each sound source to total energy which is averaged over two years, it is important to keep in mind that averaging may obscure the fact that such sudden events might potentially have a big impact at the moment they occur. We assume that transient sources can be represented as a continuous sounds (since the explosions and airgun shots were observed almost for each week at the various locations of the North Sea.) for the large time windows (over a week, month or year). They can be used to compare the annual contributions of each source to the total energy However, the shorter time windows may be required for the transients depending on the type of the biological problems.